

The Antimalarial Natural Product Symplostatin 4 Is a Nanomolar Inhibitor of the Food Vacuole Falcipains

Sara Christina Stolze,^{1,5} Edgar Deu,^{2,5} Farnusch Kaschani,^{1,5} Nan Li,⁴ Bogdan I. Florea,⁴ Kerstin H. Richau,³ Tom Colby,³ Renier A.L. van der Hoorn,³ Hermen S. Overkleeft,⁴ Matthew Bogyo,² and Markus Kaiser^{1,*}

¹Zentrum für Medizinische Biotechnologie, Fakultät für Biologie, Universität Duisburg-Essen, Universitätsstr. 2, 45117 Essen, Germany

²Department of Pathology and Department of Microbiology and Immunology, Stanford University School of Medicine, Stanford, CA 94305, USA

³Max Planck Institute for Plant Breeding Research, Carl-von-Linné-Weg 10, 50829 Cologne, Germany

⁴Faculty of Science, Leiden Institute of Chemistry, Bio-organic Synthesis, Gorlaeus Laboratories, Einsteinweg 55, 2333 CC Leiden, The Netherlands

⁵These authors contributed equally to this work

*Correspondence: markus.kaiser@uni-due.de

<http://dx.doi.org/10.1016/j.chembiol.2012.09.020>

SUMMARY

The marine natural product symplostatin 4 (Sym4) has been recognized as a potent antimalarial agent. However, its mode of action and, in particular, direct targets have to date remained elusive. We report a chemical synthesis of Sym4 and show that Sym4-treatment of *P. falciparum*-infected red blood cells (RBCs) results in the generation of a swollen food vacuole phenotype and a reduction of parasitemia at nanomolar concentrations. We furthermore demonstrate that Sym4 is a nanomolar inhibitor of the *P. falciparum* falcipains in infected RBCs, suggesting inhibition of the hemoglobin degradation pathway as Sym4's mode of action. Finally, we reveal a critical influence of the unusual methyl-methoxyproline (mmp) group of Sym4 for potent inhibition, indicating that Sym4 derivatives with such a mmp moiety might represent viable lead structures for the development of antimalarial falcipain inhibitors.

INTRODUCTION

Malaria is a devastating disease that affects approximately 215 million patients annually, among whom around 650,000 die (WHO, 2011). The spread of the disease can normally be controlled by a combination of vector control and chemotherapy. However, there is widespread resistance of the malaria parasite to most front-line therapeutics. In recent years, an emergence of resistance against artemisinin-based combination therapy, which is the standard of care recommended by the WHO for uncomplicated malaria, has furthermore been noted in Southeast Asia (Dondorp et al., 2009). Consequently, alternative chemotherapeutic strategies for combating malaria are required at a constantly increasing rate (Guiguemde et al., 2012; Wells et al., 2009).

Due to an impressive structural diversity in combination with often potent bioactivities, natural products have proven to be valuable lead structures for drug discovery (Mayer et al., 2010). Their further development into drugs is, however, often hampered by a lack of knowledge of their mode of action. Consequently, several strategies for the identification of the direct targets of bioactive natural products have been developed in the past few years (Lomenick et al., 2011; Rix and Superti-Furga, 2009). Among them, proteome labeling strategies such as activity-based protein profiling (ABPP) have evolved into reliable tools for the identification of protein targets of potentially bioactive natural small molecules (Böttcher et al., 2010; Cravatt et al., 2008; Deu et al., 2012; Heal et al., 2011; van der Hoorn et al., 2004).

In 2009, the cyanobacterial secondary metabolites symplostatin 4 (Sym4, Figure 1A) and gallinamide A were independently isolated from the species *Symploca* sp. and *Schizothrix* sp., respectively (Linnington et al., 2009; Taori et al., 2009). Subsequent total syntheses of these two natural products and structural characterizations revealed that both compounds are in fact identical (Conroy et al., 2010, 2011). Subsequent biological evaluations of Sym4 demonstrated their potent antimalarial properties: In fact, gallinamide A (and, therefore, Sym4), as well as three chemically synthesized diastereomers that differed only in the stereochemistry of their N-terminal isoleucine residue, turned out to be potent nanomolar growth inhibitors of the malaria parasite *P. falciparum* (strain 3D7 and W2, IC₅₀s of 36–100 nM) (Conroy et al., 2010, 2011; Linnington et al., 2009). Notably, no lysis of red blood cells (RBCs) was observed during Sym4 treatment even at the highest tested concentrations (>25 μM) (Conroy et al., 2010), indicating that its antiparasitic effect is not due to permeabilization of the RBC membrane. The molecular basis of this antimalarial activity, however, remained elusive.

Sym4 (Figure 1A) thereby displays several structural features that are only rarely found in natural products. For example, Sym4 features a (4S)-amino-(2E)-pentenoic acid that is linked with a methyl-methoxyproline (mmp) unit at its C-terminal end and an isocaproic acid moiety involved in an ester bond

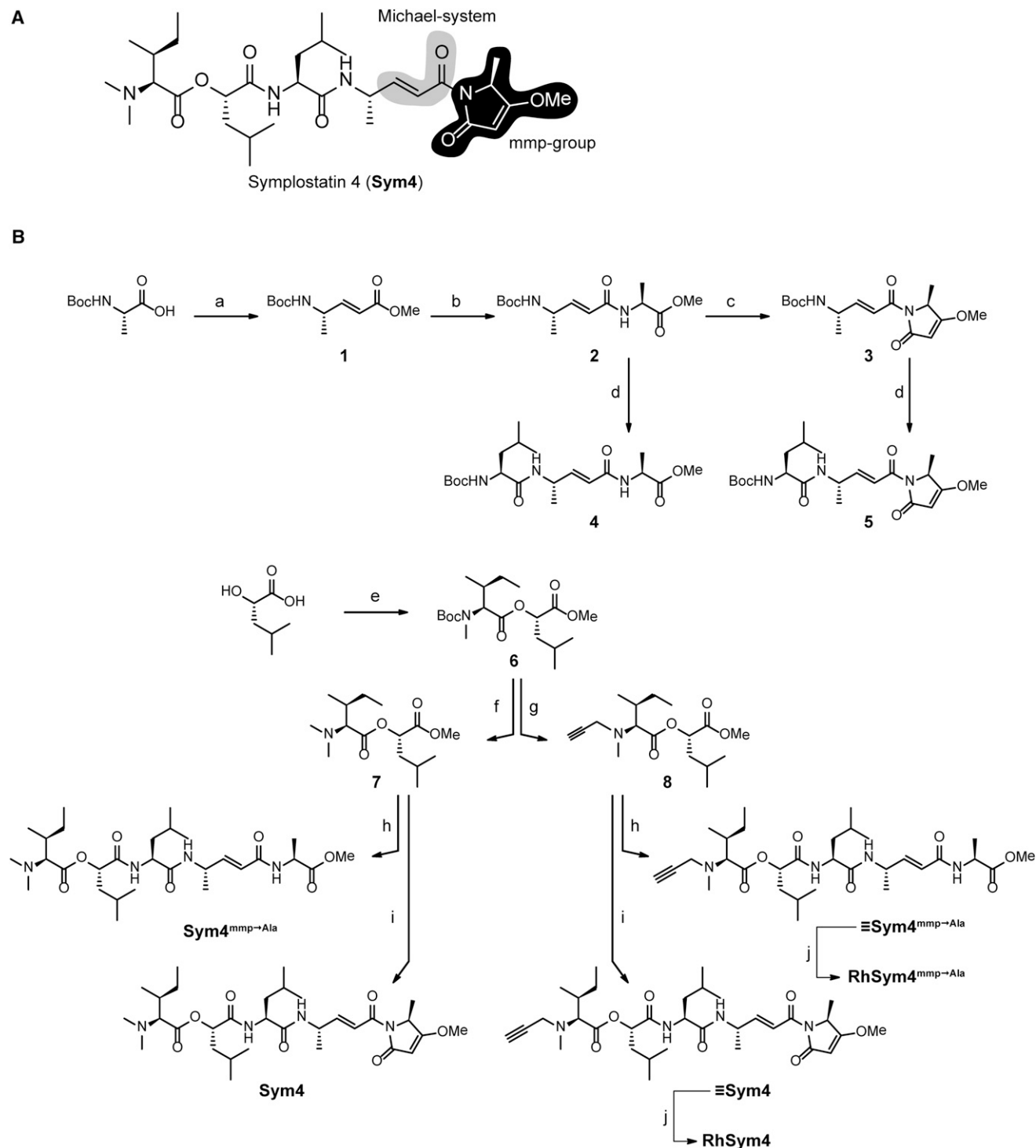


Figure 1. Structure and Synthesis of Sym4 and Sym4 Derivatives

(A) Molecular structure of the parent natural product symprostatin 4 (**Sym4**).

(B) Reagents and conditions: (a) 1. NH(OMe)Me⁺HCl, Et₃N, DCC, DCM; 2. LiAlH₄, Et₂O, (EtO)₂P(O) = CHCOOMe, DCM, 59%; (b) 1. LiOH, THF/MeOH/H₂O; 2. HAlaOMe⁺HCl, HOBT, HBTU, DIPEA, DCM, 46%; (c) 1. LiOH, THF/MeOH/H₂O; 2. Meldrum's acid, EDC, DMAP, DCM; 3. CH₃CN, reflux; 4. PPh₃, DEAD, MeOH, THF, 90%; (d) 1. TFA/DCM (1:1); 2. BocLeuOH, HOBT, HBTU, DIPEA, CH₃CN, 99% (**4**), 85% (**5**); (e) 1. SOCl₂, MeOH/DCM; 2. Boc/MelleOH, DCC, DMAP, DCM, 55%; (f) TFA/DCM (1:1); 2. MeI, DIEA, DMF, 38%; (g) TFA/DCM (1:1); 2. Propargyl bromide, DIEA, CH₃CN, 63%; (h) 1. LiOH, THF/MeOH/H₂O; 2. **4** (after cleavage with TFA/DCM [1:1]), HBTU, HOBT, DIPEA, CH₃CN, 39% (**Sym4**^{mmp→Ala}), 53% (\equiv Sym4^{mmp→Ala}); (i) 1. LiOH, THF/MeOH/H₂O; 2. **4** (after cleavage with TFA/DCM [1:1]), HBTU, HOBT, DIPEA, CH₃CN, 51% (**Sym4**), 64% (\equiv Sym4); (j) 1. LiOH, THF/MeOH/H₂O; 2. **4** (after cleavage with TFA/DCM [1:1]), HBTU, HOBT, DIPEA, CH₃CN, 23% (**RhSym4**), 67% (**RhSym4**^{mmp→Ala}).

with an N-terminally dimethylated isoleucine residue. The Michael system in the (4*S*)-amino-(2*E*)-pentenoic acid unit is, thus, potentially bioreactive (Drahl et al., 2005); in fact, covalently binding cysteine protease inhibitors, proteasome as well as GAPDH inhibitors, with such Michael acceptor units have been reported (Clerc et al., 2009a, 2009b; Groll et al., 2008; Kaschani et al., 2012; Powers et al., 2002). In **Sym4**, this chemical moiety is uniquely linked to a highly rigid mmp group, which could influence the bioreactivity and/or target specificity of this natural product.

The favorable biological activities and intriguing structural features of **Sym4** raise the question of the underlying mode of action of this antimalarial natural product. To this end, an elucidation of the direct molecular target(s) and of the structural determinants for bioactivity is highly desirable. Therefore, in the present study, we chemically synthesized **Sym4** and a set of analogs and characterized their antimalarial properties. In addition, we identified falcipains as **Sym4**'s molecular targets and investigated the role of the mmp group for bioactivity.

RESULTS

Chemical Synthesis of **Sym4** and its Derivatives

In order to obtain the required chemical probes for the target identification studies as well as for the synthesis of **Sym4** derivatives lacking the mmp group, we devised a convergent, fragment-based approach that was used to synthesize **Sym4** as well as C- and N-terminally modified **Sym4** derivatives (Figure 1; Supplemental Experimental Procedures available online). To this end, we retrosynthetically divided **Sym4** and the corresponding derivatives into two fragments, i.e., an N-terminal depsipeptide moiety and a C-terminal tripeptide residue. Such an approach is beneficial because a "combinatorial" coupling of differently modified N- and C-terminal fragments allows an efficient, cost-effective, and rapid generation of various **Sym4** derivatives.

With this plan in mind, we started our synthesis with the generation of two different C-terminal fragments that varied in the presence or absence of the mmp group (Figure 1B). Accordingly, Boc-Ala-OH was converted to an α,β -unsaturated methyl ester **1** in 59% yield using a protocol introduced by Pollini and coworkers (Benetti et al., 2002). In the next step, ester **1** was deprotected using lithium hydroxide and coupled with alanine methyl ester hydrochloride to obtain dipeptide intermediate **2**. Dipeptide **2** was deprotected C-terminally with lithium hydroxide and the resulting intermediate was coupled with Meldrum's acid, yielding a highly reactive enol intermediate that rearranged into a pyrrolidine-2,4-dione moiety upon reflux in acetonitrile. The use of Mitsunobu conditions (DEAD, methanol, and triphenylphosphine) then transformed this pyrrolidine-2,4-dione into the desired mmp-modified dipeptide **3** in 90% yield (Patino et al., 1992). The final C-terminal tripeptide building block **5** was then obtained in 85% yield by Boc deprotection of **3**, followed by a coupling step with Boc-Leu-OH and HBTU/HOBt activation and acetonitrile as the solvent (Jou et al., 1997). In contrast, the tripeptide building block **4** that lacks a mmp group but features, instead, an alanine residue was obtained by acidic Boc deprotection of **2** and subsequent coupling of the free amine to Boc-Leu-OH, again with

HBTU/HOBt activation and acetonitrile as the solvent (Jou et al., 1997).

The two different N-terminal depsipeptide fragments—i.e., one building block with an N-dimethylated isoleucine residue (**7**) and the other one with an N-methyl-propargyl-modified isoleucine moiety (**8**)—were synthesized next. To this end, (S)-2-hydroxy-isocaproic acid was converted into a methyl ester and coupled with N-methylated Boc-isoleucine, thereby yielding the desired depsipeptide **6**. The Boc group was cleaved and the resulting intermediate modified at its N-terminal amino group with either a methyl (**7**) or a propargyl group (**8**).

For fragment assembly, the corresponding N- and C-terminal building blocks were then coupled with each other. Accordingly, the N-terminal dipeptide fragments **7** and **9** were first C-terminally deprotected by saponification with lithium hydroxide and then directly coupled to the Boc-protected C-terminal tripeptide fragments **4** or **5**, using HBTU/HOBt activation. This approach delivered the desired natural product **Sym4** (51%) and the derivatives for structure-activity relationship studies (i.e., the alkyne-tagged derivative \equiv **Sym4** [64%] as well as the corresponding **Sym4**^{mmp→Ala} [39%] and \equiv **Sym4**^{mmp→Ala} [53%] derivatives without the mmp group).

Finally, the propargyl-modified analogs \equiv **Sym4** and \equiv **Sym4**^{mmp→Ala} were tagged with a rhodamine fluorophore, using a Cu⁺-mediated Huisgens [3+2] cycloaddition and Rh-N₃ (Kolb et al., 2001; Speers et al., 2003). This approach resulted in the generation of two fluorescent probes **RhSym4** and **RhSym4**^{mmp→Ala} that were later used in the ABPP experiments.

Biological Assays Reveal the Critical Role of the mmp Group of **Sym4** for Antimalarial Activity

With these compounds in hand, we first evaluated the effect of **Sym4** and **Sym4**^{mmp→Ala} on malaria parasite replication during the erythrocytic cycle. To this end, a culture of *P. falciparum* D10 parasites at ring stage and 2% parasitemia was treated for 75 hr (i.e., one and a half life cycles) with different concentrations of **Sym4** and **Sym4**^{mmp→Ala} (Figure 2A). After 75 hr, the parasites reached schizont stage with completed DNA replication, thereby allowing an efficient differentiation between infected and noninfected RBCs via propidium iodide staining and subsequent parasitemia quantification via flow cytometry as described previously (Deu et al., 2010). **Sym4** (EC₅₀ = 0.7 ± 0.2 μM) was 40-fold more potent than **Sym4**^{mmp→Ala} (EC₅₀ = 27 ± 7 μM), indicating that the C-terminal mmp group significantly contributes to the antiparasitic activity of this compound.

In order to better understand the mechanism of action of **Sym4**, we next investigated whether treatment with these compounds induces a specific phenotype. To this end, ring stage parasites were treated with different concentrations of **Sym4** and **Sym4**^{mmp→Ala}. After 24 hr, their morphology was visualized by Giemsa-stained thin blood smears. In this assay, cells treated with 0.1 μM **Sym4** already showed a distinct swollen food vacuole phenotype (Figure 2B, upper panel). On the other hand, a 100-fold higher concentration of **Sym4**^{mmp→Ala} was required to cause the same effect (Figure 2B, lower panel). In many cases, such a phenotype is caused by accumulation of nondigested hemoglobin or oligopeptides in the food vacuole, generally due to inhibition of proteases involved in this pathway

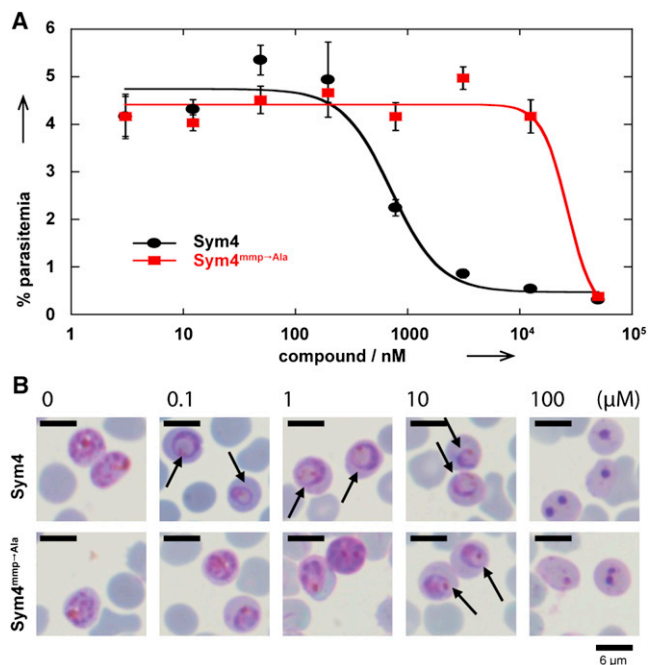


Figure 2. Comparison of the Biological Activities of *Sym4* and *Sym4*^{mmp→Ala}

(A) ***Sym4*** inhibits *P. falciparum* growth at ring stage with an $EC_{50} = 0.7 \pm 0.2 \mu\text{M}$ and thus at significantly lower concentrations than ***Sym4*^{mmp→Ala}** ($EC_{50} = 27 \pm 7 \mu\text{M}$). Error bars indicate SD from three independent experiments.

(B) ***Sym4*** induces a swollen food vacuole phenotype (indicated by arrows) at concentrations as low as 0.1 μM , thereby indicating inhibition of the hemoglobin degradation pathway (Rosenthal, 2004, 2011). Intriguingly, ***Sym4*^{mmp→Ala}**, the ***Sym4*** derivative with alanine instead of the methylmethoxypropylrolinone unit, requires concentrations of 10 μM to achieve the same phenotype.

See also Figure S1.

(Rosenthal, 2004, 2011). In fact, two distinct food vacuole defects have been reported in the literature: (1) A red swollen food vacuole that is observed when proteases involved at the initial stages of hemoglobin degradation are inhibited (falcipains 2/2/3). This results in an accumulation of undigested hemoglobin that still contains the heme group (red color). (2) A clear swollen food vacuole was recently reported due to an inhibition of aminopeptidases (Harbut et al., 2011), which does not block the initial breakdown of hemoglobin but results in the accumulation of undigested peptides (clear). In the case of ***Sym4*** treatment, we observed a red food vacuole defect, which indicates that ***Sym4*** blocks the initial stages of hemoglobin degradation. We did not observe lysis of RBCs with either of the two compounds, which is in accordance with previously published data (Conroy et al., 2010). Finally, a dead phenotype was observed at 100 μM (Figure 2B). This is most likely due to a general toxic effect caused by the reactivity of the (4S)-amino-(2E)-pentenoic acid unit found in this class of compounds.

To determine whether ***Sym4*** had any effect on parasite egress from infected RBCs or erythrocyte invasion, we then treated trophozoites for 24 hr with different concentrations of ***Sym4*** and analyzed the parasites morphology by Giemsa-stained thin blood smears (Figure S1). No effects were observed below

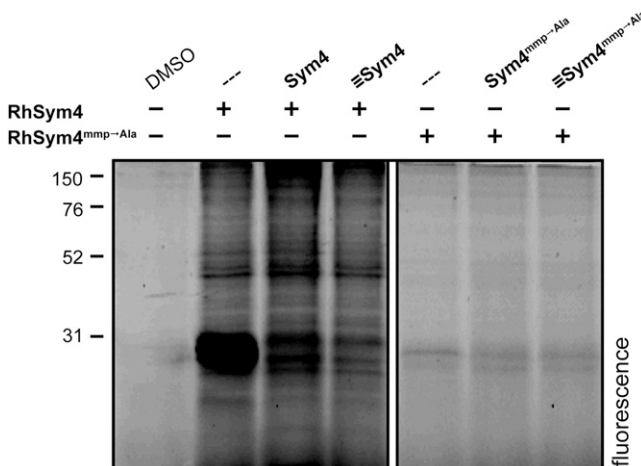


Figure 3. Labeling Pattern of *RhSym4* and *RhSym4*^{mmp→Ala}

Labeling of intact parasites with ***RhSym4*** and ***RhSym4*^{mmp→Ala}**. Purified schizonts were pretreated with 10 μM of the nonfluorescent compounds ***Sym4***, **\equiv *Sym4***, ***Sym4*^{mmp→Ala}**, **\equiv *Sym4*^{mmp→Ala}**, or DMSO. This was followed by 1 hr incubation with 10 μM ***RhSym4*** or ***RhSym4*^{mmp→Ala}**. The labeling reaction was stopped by boiling the samples in gel electrophoresis loading buffer. Proteins were resolved by SDS-PAGE and fluorescent proteins were visualized with a flatbed fluorescence scanner. The figure was assembled using two regions of the same gel. Lanes irrelevant to the conclusion were omitted (indicated by white box).

See also Figures S3 and S4.

10 μM . However, at concentration of 10 μM and above an accumulation of mature schizonts was observed (Figure S1). This effect was not permanent as these parasites were able to egress and invade RBCs normally if cultured for another 24 hr in the presence of ***Sym4*** (Figure S1). Therefore, we assume that this delay in rupture results from an inhibition of the hemoglobin degradation by ***Sym4***, which is known to slow down parasite development.

Labeling of Infected Blood Samples with *RhSym4* Reveals One Major Target for *Sym4*

To clarify whether ***Sym4*** covalently modifies its targets, we compared the labeling patterns of *P. falciparum*-infected blood samples treated with ***RhSym4*** and ***RhSym4*^{mmp→Ala}**. To this end, intact schizonts were incubated with the rhodamine-modified compounds in the presence or absence of their respective nonfluorescent derivatives. After incubation, proteins were isolated and resolved by denaturing PAGE, and the fluorescently labeled proteins were visualized using a flatbed fluorescence scanner (Figure 3). In the case of ***RhSym4***, two strongly labeled protein bands in the 28 kDa region became visible. The labeling event was sensitive to preincubation with the natural product ***Sym4***, as well as with the closely related analog **\equiv *Sym4***, indicating that the interaction is indeed dependent on the structure of the compounds and not an artifact caused by the rhodamine group. On the other hand, the same experiment with ***RhSym4*^{mmp→Ala}** revealed only weak labeling in the 28 kDa region. Importantly, these results correlate well with the different potency of ***Sym4*** and ***Sym4*^{mmp→Ala}** in the parasite assays (Figures 2A and 2B).

Competitive Activity-Based Protein Profiling Identifies Falcipains as *Sym4* Targets

The formation of a food vacuole defect by *Sym4*, the known bio-reactivity of vinyl amino acid derivatives toward cysteine proteases, and the labeling of proteins at 28 kDa by *RhSym4* strongly suggested that one or more of the food vacuole's falcipains (FP2, FP2', and FP3) (Rosenthal, 2004, 2011) might be targets of *Sym4*. These proteases are plasmodial papain-like cysteine proteases (PLCPs) that are known to migrate at 28 kDa in an SDS-PAGE and are important for the proper development of the parasite in the blood stages (Greenbaum et al., 2002b; Pandey et al., 2006). FP1 is the only falcipain outside of the food vacuole and is believed to play a role in RBC invasion (Greenbaum et al., 2002b). FP2, FP2', and FP3 are involved in the hemoglobin degradation pathway, which is the main source of amino acids for the developing parasite (Sijwali and Rosenthal, 2004). Importantly, inhibition of these three proteases causes the same phenotype as the one observed for *Sym4* treatment (i.e., a swollen food vacuole and block of parasite replication; Figure 2) (Moura et al., 2009; Rosenthal et al., 1988). The phenotype observed with *Sym4* is also reminiscent of the initial phenotype reported for the *P. falciparum* FP2 knockout strain. Parasites lacking FP2 undergo a transient food vacuole swelling at trophozoite stage that resolves in the schizont stage due to concomitant expression of FP3 (Sijwali and Rosenthal, 2004; Sijwali et al., 2006).

In order to probe if *Sym4* targets falcipains 2, 2', and 3, we performed competitive ABPP experiments with the activity-based PLCP probe Cy5-DCG-04 (Greenbaum et al., 2000). In competitive ABPP experiments, biological samples are first pre-incubated with the small-molecule inhibitors of interest, followed by visualization of residual enzyme activity by a fluorescent probe (Clerc et al., 2011; Cravatt et al., 2008; Fonović and Bogyo, 2008; Jeffery and Bogyo, 2003). In general, such an approach allows the evaluation of inhibitory potency and specificity under physiologically relevant conditions.

To this end, parasite lysates were incubated first with different concentrations of *Sym4* or *Sym4*^{mmp→Ala} and then labeled with Cy5-DCG-04. Subsequently, proteins were separated by electrophoresis and visualized by in-gel fluorescence detection (Figure 4A). The advantage of using Cy5-DCG-04 is that its targets in *P. falciparum*-infected RBCs have already been identified in previous studies (Greenbaum et al., 2002a, 2002b; Pandey et al., 2006). Therefore, a reduction in the intensity of one of the known signals reveals this PLCP as a target of the tested compounds. Satisfyingly, *Sym4* was found to be an astonishingly potent inhibitor of FP2, FP2', and FP3, inhibiting these proteases at low nanomolar concentrations (1.5 nM). FP1 was also inhibited, but at significantly higher concentrations (>1.6 μM). In contrast, *Sym4*^{mmp→Ala} proved to be much less potent, inhibiting Cy5-DCG-04 labeling of FP2, FP2', and FP3 only at concentrations above 25 μM, while no inhibition of FP1 labeling was observed. Interestingly, ≡*Sym4* and ≡*Sym4*^{mmp→Ala} showed an inhibition pattern similar to their corresponding parent compounds (Figure S2), indicating that the N-terminal part of the protein is not essential for target inhibition.

Another class of plasmodial PLCPs is the dipeptidyl aminopeptidases (DPAPs). DPAP1 and DPAP3 are essential cysteine

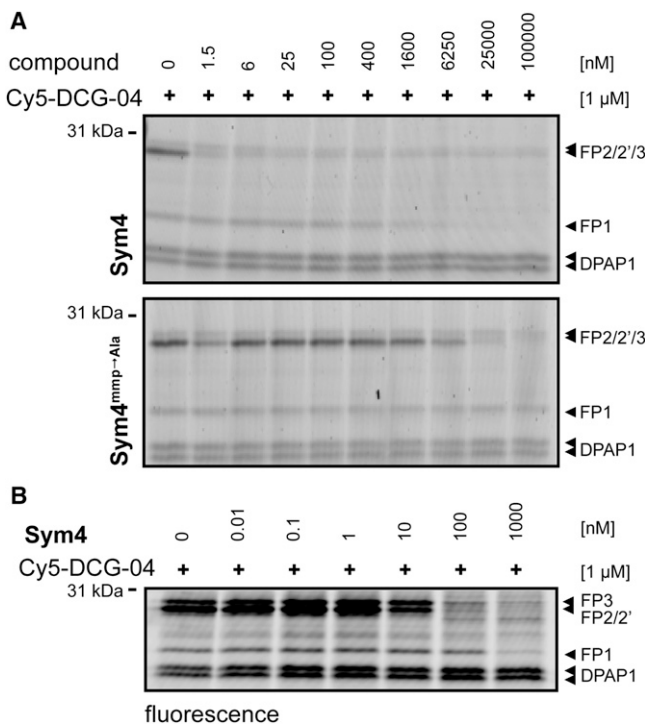


Figure 4. Characterization of *Sym4* Specificity Using Activity-Based Protein Profiling with Cy5-DCG-04

(A) *P. falciparum* D10 lysates (in 50 mM NaOAc, pH 5) were preincubated for 30 min with different concentrations of *Sym4* or *Sym4*^{mmp→Ala}, followed by addition of 1 μM Cy5-DCG-04. After 1 hr, the reaction was stopped by adding SDS-PAGE loading buffer and boiling for 5 min. Proteins were resolved by SDS-PAGE and visualized by in-gel detection of fluorescence on a flatbed fluorescence scanner. *Sym4* inhibited FP2/2'/3 at low nanomolar concentrations and FP1 at concentrations above 1.6 μM. In contrast, *Sym4*^{mmp→Ala} was a much weaker FP2/2'/3 inhibitor and did not inhibit FP1 at the concentrations used. DPAP1, dipeptidyl aminopeptidase 1 (Arastu-Kapur et al., 2008; Greenbaum et al., 2002b).

(B) *Sym4* inhibits the falcipains in living parasite. A culture of *P. falciparum* at trophozoite stage was treated for 1 hr with different concentrations of *Sym4*. Parasite pellets were separated from RBCs by saponin lysis and residual PLCP activities were measured by lysing the pellets in acetate buffer containing 1% NP40 and 1 μM of Cy5-DCG-04. After 1 hr, the reaction was stopped by adding SDS-PAGE loading buffer. Proteins were resolved by SDS-PAGE and visualized by in-gel detection of fluorescence on a flatbed fluorescence scanner. *Sym4* inhibited falcipains 1, 2/2', and 3 at high, low, and medium nanomolar concentrations ($IC_{50}^{FP1} = 140 \pm 23$ nM, $IC_{50}^{FP2/2'} = 8.5 \pm 1.3$ nM, $IC_{50}^{FP3} = 22 \pm 8$ nM), respectively. *Sym4* did not inhibit DPAP1 at 1 μM. See also Figures S2–S5.

proteases during the erythrocytic cycle and are involved in hemoglobin degradation (Klemba et al., 2004; Deu et al., 2010) and parasite egress (Arastu-Kapur et al., 2008), respectively. Competitive ABPP with either the probe Cy5-DCG04 or the DPAP activity-based probe FY01 showed that neither DPAP1 (Figure 4) nor DPAP3 (Figure S3) is inhibited by *Sym4*. Consequently, these experiments indicate that *Sym4* does not act as a general inhibitor of *P. falciparum* cysteine proteases but rather preferentially inhibits food vacuole falcipains.

After these encouraging results, we turned our attention to the determination of the inhibition potency of *Sym4* in intact parasites. To this end, purified schizonts were treated with different

concentrations of **Sym4** for 1 hr, RBCs were lysed with saponin, and the residual activity of PLCPs in the parasite pellets was again labeled with Cy5-DCG-04 (Figure 4B). This assay confirmed that **Sym4** is a nanomolar inhibitor of falcipains in intact parasites, although this time we also observed potent inhibition of FP1. Quantification of the gel labeling pattern thereby revealed a preferential inhibition of FP2/2' over FP3 or FP1 ($IC_{50}^{FP2/2'} = 8.5 \pm 1.3$ nM, $IC_{50}^{FP3} = 22 \pm 8$ nM, $IC_{50}^{FP1} = 140 \pm 23$ nM; Figure 4B).

To further characterize the inhibitory potency of **Sym4**, we subsequently determined the kinetics of substrate turnover inhibition, using recombinantly produced FP2 or FP3 at different inhibitor concentrations (Figure S5). As expected, this experiment confirmed that **Sym4** is an irreversible inhibitor of these two falcipains. Moreover, and in accordance with the competitive ABPP experiments, FP2 turned out to be more potent than FP3 (FP2: $k_i = k_{obs} / [I] = 58,600 \pm 1,400$ M⁻¹s⁻¹ versus FP3: $k_i = k_{obs} / [I] = 7,030 \pm 250$ M⁻¹s⁻¹).

In order to evaluate the bioreactivity pattern of **Sym4**, we next investigated if **Sym4** also inhibits mammalian PLCPs or the proteasome. To this end, we performed additional competitive ABPP experiments with bone marrow-derived mouse macrophages in vivo. This mammalian cell line was preincubated with 0.5 μM and 5 μM of **Sym4**, ≡**Sym4**, **Sym4**^{mmp→Ala}, or ≡**Sym4**^{mmp→Ala}. Then, selected residual protease activities were determined by incubating protein extracts with a broad-band PLCP ABP (Greenbaum et al., 2002a) (Figures S4A and S4B) or with a proteasome-specific ABP (Kolodziejek et al., 2011) (Figures S4C and S4D). In these assays, **Sym4**, ≡**Sym4**, **Sym4**^{mmp→Ala}, or ≡**Sym4**^{mmp→Ala} did not inhibit the proteasome (Figures S4C and S4D). In contrast, we observed a concentration-dependent inhibition of cathepsins in these experiments. Both **Sym4** and ≡**Sym4** were found to inhibit cathepsin L at 0.5 μM (Figure S4A). At the 5 μM concentration, cathepsins B, H, S, and Z were also inhibited. As observed with the falcipains, the **Sym4** derivatives lacking the mmp group were less active. **Sym4**^{mmp→Ala} or ≡**Sym4**^{mmp→Ala} did not inhibit any cathepsins at 0.5 μM, but did inhibit cathepsin L at 5 μM (Figure S4B). We then tested the labeling properties of the fluorescent probes **RhSym4** and **RhSym4**^{mmp→Ala} also with bone marrow-derived mouse macrophages (Figure S4E). Interestingly, the obtained labeling profile indicates, as expected from the competitive ABPP experiments, that the predominant target of **Sym4** in mammalian cells is cathepsin L.

DISCUSSION

Half of the human population is threatened by malaria, and the urge to develop novel antimalarial therapies is becoming more and more pressing (Guiguemde et al., 2012). Compounds with antimalarial activity are frequently reported in the literature (Nogueira and Lopes, 2011), but further development of these compounds into drugs is often hampered by their difficult chemical synthesis (or limited availability via natural product isolation) and/or their unknown mode of action.

The natural product symplostatatin 4 (**Sym4**) has been identified as another promising antimalarial compound (Conroy et al., 2010, 2011). To investigate the mode of action of this promising antimalarial agent, we synthesized several analogs to (1) identify

its direct molecular targets and (2) characterize the underlying structure-activity relationships and correlate them to the antimalarial activities.

Synthesis of Sym4 and Derivatives

We first developed a convergent synthesis to **Sym4** and derivatives. In order to establish a synthetic route that allows rapid access to different **Sym4** derivatives, a modular synthesis was devised. Thus, in contrast to previous synthetic approaches, which relied on a stepwise assembly of different amino acid building blocks, we chose a fragment condensation strategy to assemble the **Sym4** framework. Consequently, two different N- and C-terminal fragments were synthesized via solution phase peptide synthesis and merged to four different **Sym4** derivatives. This approach was used to synthesize not only the natural product **Sym4**, but also derivatives lacking the C-terminal mmp group. In addition, derivatives with a propargyl group at the N terminus were generated, which enabled the attachment of a fluorescent reporter rhodamine via a copper-catalyzed click reaction in an additional reaction step (**RhSym4** and **RhSym4**^{mmp→Ala}).

Altogether, the developed synthetic route allows a rapid and facile generation of **Sym4** and derivatives, using “standard” peptide chemistry manipulations. However, because malaria mostly affects people in third world countries that cannot afford expensive medication, the cost of goods of a synthesis is always an important issue. Although the prices for the required starting materials (i.e., mainly amino acids and other peptide chemistry reagents) have decreased significantly in the last few years, the overall costs of the chemical synthesis of **Sym4** derivatives, even if established on an industrial scale, will most probably exceed the generally accepted \$2 limit. Thus, for a chemotherapeutic utilization of **Sym4**, further compound optimization, in regard not only to its bioactivities but also to the cost of synthesis, is still required; along these lines, **Sym4** derivatives featuring a structurally less complex N-terminal fragment but maintaining the biologically relevant C-terminal moieties might be more appropriate drug candidates.

Falcipain Inhibition Is Responsible for the Antimalarial Activity of Sym4

The evaluation of the biological activity of chemically synthesized **Sym4** confirmed that this natural product is a potent antimalarial compound, as was previously reported (Conroy et al., 2010, 2011). In phenotypic assays, we subsequently showed that **Sym4** causes a distinct food vacuole defect at nanomolar concentrations (Figure 2). These findings guided our following target identification studies using competitive ABPP, which demonstrated all four *P. falciparum* falcipains as targets of **Sym4** in intact parasites. However, we observed different inhibition potencies: **Sym4** most potently inhibited FP2/2', followed by FP3 and FP1. Among the different falcipains, FP3 is the only one for which knockout attempts have been unsuccessful, which suggests it is the most important falcipain during *P. falciparum* blood stages. FP1 and FP2' knockout strains have no apparent phenotype, with FP1 not being essential in the erythrocytic stage of malaria (Sijwali et al., 2004), while the FP2 knockout showed a marked food vacuole defect (Sijwali et al., 2004; Sijwali and Rosenthal, 2004). To the best of our knowledge, the FP2/2'

double knockout has not been attempted, so we cannot rule out that inhibition of both FP2 homologs is lethal to parasites. With this caveat in mind, our findings suggest that FP3 inhibition might be the crucial factor for the antimalarial activity of **Sym4**. Although we observed the formation of a food vacuole defect at 0.1 μM **Sym4**, parasite killing (i.e., the antimalarial activity) required 7-fold higher concentrations ($\text{EC}_{50} = 0.7 \mu\text{M}$). The different concentrations required to induce parasite killing on the one hand, and the formation of the food vacuole defect on the other hand, might at least partly result from the falcipain inhibition profile of **Sym4**. Although at lower concentrations **Sym4** first inhibits FP2/2' and thus causes a food vacuole phenotype, higher concentrations are required for supplementary FP3 inhibition, thereby inducing parasite killing. In any case, it is important to note that **Sym4** inhibits falcipains in intact parasites with IC_{50} s in the low to medium nanomolar range, which is much lower than the observed EC_{50} of 0.7 μM in the replication assay. Several reasons might explain the discrepancy between these two values. First, high fractional and sustained inhibition of falcipains might be required to impair parasite replication. This has been observed for DPAP1, where sustained inhibition of more than 90% of DPAP1 activity for several hours is required to effectively block parasite replication (Deu et al., 2010). Therefore, the required concentrations of **Sym4** for impairing *P. falciparum* replication via inhibition of falcipains needs to be much higher than the actual IC_{50} value. The fact that **Sym4** does not irreversibly block egress also indicates that **Sym4** does not inhibit other cysteine proteases involved in schizont rupture, such as DPAP3 (Figure S3) or human calpain-1 (Chandramohanadas et al., 2011; Millholland et al., 2011). Second, the intramolecular **Sym4** concentration and thus the "reservoir" of "free" **Sym4** that is available to target falcipains might be lower than anticipated, thereby resulting in less efficient falcipain inhibition. Several mechanisms might lead to such a reduced **Sym4** concentration. For example, although our studies indicate that falcipains are cell permeable, the uptake of extracellular **Sym4** into the cytosol might be hampered or slowed down. In addition, it is reasonable to assume that off-target binding to other proteins or cell components reduce the amount of "free" **Sym4**; although some of these binding events might be reversible, the reaction of **Sym4** with host cathepsins such as cathepsin L (Figure 4A), for example, is most probably irreversible, thereby persistently reducing **Sym4** levels. Finally, intracellular **Sym4** might also be metabolically or chemically unstable and thus intracellular **Sym4** levels could be subject to a continuous decline. Interestingly, in our replication assay parasites were treated at ring stage, while for example FP3 is known to be expressed at schizont stage (i.e., more than 24 hr after treatment). At this point, **Sym4** concentration may already be significantly reduced, thereby explaining the observed bioactivity difference between falcipain inhibition in intact parasites and the EC_{50} on infected red blood cells.

Despite these drawbacks, our experiments revealed **Sym4** as one of the most potent falcipain inhibitors reported so far (Teixeira et al., 2011). This potency is accompanied by a distinct selectivity pattern. By performing comparative ABPP experiments with a specific proteasome probe in living cells (MVB003), we could verify that **Sym4** does not inhibit the mammalian proteasome at concentrations up to 5 μM (highest

tested concentration; Figure S4C). However, a similar assay testing for activity against mammalian cathepsins using BODIPY-DCG04 (Greenbaum et al., 2002a) showed that **Sym4** also reacts with mammalian cathepsins. Our assays indicated that among the different cathepsins, **Sym4** preferentially reacts with cathepsin L. In an uninfected mammalian cell line, **Sym4** inhibits a large portion of cathepsin L at a concentration of 0.5 μM and thus at a concentration comparable to the observed antimalarial effect of **Sym4**. In contrast, the cathepsins B, H, S, and Z required ten times higher concentrations (i.e., 5 μM) to reach the same inhibition level (Figure S4A). Although the observed "off-target" inhibition of cathepsin L is not desirable, a recent report indicated that only a high fractional inhibition of cathepsins (i.e., more than 95% inhibition) leads to a considerable biological effect (Méthot et al., 2008). Nevertheless, these findings indicate that further studies are required to evaluate the impact of off-target cathepsin inhibition for the further utility of **Sym4** as a guiding structure for the development of antimalarials.

Finally, as a spin-off of our studies, we observed that the synthesized rhodamine analog **RhSym4** strongly labels the food vacuole falcipains in intact parasites (Figure 3). To the best of our knowledge, this is the first activity-based probe that discriminates between the food vacuole falcipains and FP1, and the first fluorescent activity-based probe that labels FP2, 2', and 3 in intact cells. Therefore, development of probes based on the **Sym4** scaffold might prove to be very useful tools for imaging PLCP activity in cells.

The mmp Group Is Critical for Efficient Inhibition of Falcipains

In order to better understand the structure-activity relationship of **Sym4**, we tested different N- and C-terminal derivatives for their antimalarial activity. We found that changes at the N-terminal end were well tolerated and had only a slight effect on bioactivity. For example, the \equiv **Sym4** derivative showed a similar inhibition pattern as **Sym4** (Figures S2 and S4B). These findings indicate that the N-terminal part of **Sym4** is amenable for at least slight modifications and not essential for target recognition. These findings are indeed corroborated by previous synthetic studies of **Sym4** derivatives (Conroy et al., 2010, 2011).

On the other hand, replacement of the C-terminal mmp group with an alanine (**Sym4**^{mmp→Ala}) results in severe loss of antimalarial potency. This is very interesting because the mmp group is rarely found in natural products, and most falcipain inhibitors reported so far have peptide-like structures at the C-terminal end, similar to the **Sym4**^{mmp→Ala} derivative. In parasite assays, **Sym4**^{mmp→Ala} proved to be a much weaker inhibitor of the falcipains than **Sym4** (Figure 4), which explains its reduced antimalarial activity (Figure 2). Furthermore, our results indicate that the mmp group has a decisive influence on not only the potency of falcipain inhibition, but also for other PLCPs (Figures S4A and S4B). Although we have not further investigated the molecular basis of the different activity patterns, we anticipate that different factors might contribute to the observed increase of activity. For example, the mmp group might occupy a distinct binding pocket in the active site of falcipains. The resulting increase in binding affinity and thus local concentration of **Sym4** would consequently favor the subsequent irreversible reaction with the active

site cysteine, resulting in an overall improved inhibition rate. Alternatively, the mmp group may also increase the overall chemical reactivity of **Sym4**. In fact, we observed a stronger background labeling for **RhSym4** versus **RhSym4^{mmp→Ala}** (Figure 3), suggesting that higher chemical reactivity may contribute to the improved inhibition rate. On the other hand, it has been frequently noticed that attaching fluorescent groups like rhodamine or BODIPY to electrophiles like Michael systems or epoxides increases the off-target labeling of these ABPs when compared to strictly biotinylated ABPs. Taken together, the mmp group enhances the overall falcipain inhibition rate but may also increase off-target effects. Therefore, future chemical derivatizations of the **Sym4** structure aiming at the improvement of its inhibitory potential will have to be complemented by selectivity studies.

Finally, it is important to note that falcipains have been recognized as potential targets for the development of antimalarials for quite some time, and numerous compound classes have evolved that address these enzymes (Teixeira et al., 2011). Among them, peptidic small molecules featuring an electrophilic warhead such as epoxides or Michael acceptor systems have proven to be potent inhibitors. Despite intense efforts, none of these compounds could be developed into a drug and, therefore, interest in falcipain inhibitors has slightly decreased in the last few years. **Sym4** is also based on an α,β -unsaturated Michael acceptor system that is, however, C-terminally linked to a mmp group, resulting in a structurally novel scaffold that has, so far, not been investigated. Indeed, our findings indicate that this unusual combination results in much more potent inhibitors, suggesting that further studies, for example with N-terminally modified, less peptidic derivatives, might represent a feasible approach to finally tackle these drug targets.

SIGNIFICANCE

In summary, we have reported a total synthesis of Sym4 and the rational synthesis of a series of analogs. Sym4 causes a food vacuole phenotype in Plasmodium-infected RBCs and inhibits pathogen replication with an EC₅₀ of 0.7 μ M. We subsequently identified the falcipains as direct molecular targets of Sym4, thereby explaining its potent antimalarial properties. Finally, we elucidated the C-terminal mmp unit as a critical component for potent inhibition of falcipains. Therefore, our findings not only provide the mechanistic basis for the observed potent antimalarial properties of the marine natural product symplostatin 4 (Sym4), but they may also serve as a valuable guide for the future rational design of potent falcipain inhibitors. Although an assessment of the drug-like properties of Sym4 has yet to be done, we anticipate that the synthesis of Sym4-like derivatives opens new possibilities to the design of tool compounds to investigate and develop antimalarial chemotherapeutics that combat this devastating disease.

EXPERIMENTAL PROCEDURES

Parasite Culture, Harvesting, and Lysate Preparation

D10 *P. falciparum* were cultured and kept synchronous as previously described (Arastu-Kapur et al., 2008). Trophozoite stage parasites were

harvested 36 hr postinvasions. Parasites were released and isolated from RBCs after saponin lysis of the RBC membrane. Proteins were extracted from parasites by treatment with PBS containing 1% NP40. The soluble fraction was subsequently separated from the insoluble one by centrifugation (Arastu-Kapur et al., 2008).

Phenotypic Characterization of Sym4-Treated Parasites

A synchronized culture of the parasite at ring stage (2% parasitemia) was treated with different concentrations of **Sym4**, **Sym4** analogs, or DMSO. After 24 hr, phenotypic effects were observed by Giemsa-stained thin blood smears. The food vacuole defect is clearly visible as an enlargement of this acidic organelle. This is due to the inhibition of proteases in the food vacuole that leads to the accumulation of undigested hemoglobin.

P. falciparum Replication Assay

A total of 200 μ l synchronous D10 parasites at ring stage (2% parasitemia and 0.5% hematocrit) were treated with the corresponding compounds and cultured in 96-well plates for 75 hr until the DMSO controls reached schizont stage. Quantification was performed by flow cytometry as previously described (Wang et al., 2011). All fluorescence activated cell sorting measurements were taken on a BD FACScan flow cytometer (Becton Dickinson). EC₅₀ values for parasite death were obtained by fitting the parasitemia values to a dose-response curve.

Labeling of Cysteine Protease Activity with ABPs and Competition of Labeling by Protease Inhibitors

Cy5-DCG04, a cell-impermeable fluorescently tagged activity-based probe was used to label the activity of DPAP1 and falcipains in lysates. To test the potency of **Sym4** and analogous compounds, parasite lysates (diluted 1:10 in acetate buffer [50 mM sodium acetate, 5 mM MgCl₂, and 5 mM DTT at pH 5.5]) were pretreated with the corresponding compounds for 30 min followed by labeling for 1 hr with 1 μ M of Cy5-DCG04. The reaction was stopped by boiling the samples in SDS-PAGE loading buffer. Proteins were resolved by SDS-PAGE and the different cysteine proteases were detected using a Typhoon 9410 flat-bed fluorescence scanner (Amersham Biosciences, GE Healthcare).

Labeling of proteins from intact parasites with **RhSym4** and **RhSym4^{mmp→Ala}** was performed by incubating purified schizonts with different concentration of **RhSym4** for 1 hr in PBS followed by boiling of the samples in loading buffer and separation of the different proteins by SDS-PAGE. Labeled bands were detected using the Typhoon 9410 scanner.

To measure falcipain inhibition in living parasites, a culture of *P. falciparum* at 20% parasitemia and 2% hematocrit was treated with different concentrations of **Sym4**. After 1 hr of treatment, a 1 ml aliquot of culture was lysed with 0.15% saponin in PBS buffer, the parasite pellets were harvested, and residual cysteine protease activity was detected by labeling with 1 μ M of Cy5-DCG04 for 1 hr in acetate buffer containing 1% NP40. After SDS-PAGE, the labeling of FP1, FP2/2', FP3, and DPAP1 was quantified using the ImageJ software (Abrámoff et al., 2004) and fitted to a sigmoidal dose response curve to obtain IC₅₀ values.

K_i Determination Using a Biochemical Activity Assay for FP2 and FP3

Inhibition values of recombinantly produced FP2 and FP3 were measured at 25°C in assay buffer (200 mM sodium acetate, 10 mM DTT, 0.01% Triton-X, 3.625% glycerol, pH 6) containing 25 μ M of Z-LR-AMC. Substrate turnover was measured for 2 hr in a 96-well plate at 460 nm ($\lambda_{\text{excitation}} = 350$ nm and an emission cutoff filter at 435 nm) in a Spectramax M5 plate-reader (Molecular Devices).

Accurate k_i values (corresponding to $k_{\text{obs}} / [I]$) for **Sym4** (second order rate constant of inhibition) were obtained by incubation of FP2 or FP3 with different concentrations of **Sym4** and by recording the decrease in activity over time. The rates of substrate turnover relative to the DMSO controls (v/v_0) were fitted to a simple irreversible inhibitor model:



$$\frac{v}{v_0} = \exp(-k_{\text{obs}} \cdot [I] \cdot t).$$

Synthesis of Sym4 and Sym4 Derivatives

The synthesis and characterization of compounds **1** to **8** as well as **Sym4** and **Sym4** derivatives are described in [Supplemental Experimental Procedures](#).

SUPPLEMENTAL INFORMATION

Supplemental Information includes five figures and Supplemental Experimental Procedures and can be found with this article online at <http://dx.doi.org/10.1016/j.chembiol.2012.09.020>.

ACKNOWLEDGMENTS

The authors would like to thank Dr. Rosenthal for providing recombinant FP2 and FP3. This research was funded by the Max Planck Society and the Deutsche Forschungsgemeinschaft HO 3983/4-1 (to R.H.), by an ERC starting grant (No. 258413, to M.K.), and NIH Grants R01EB005011 and R01AI078947 (to M.B.).

Received: April 23, 2012

Revised: September 5, 2012

Accepted: September 27, 2012

Published: December 20, 2012

REFERENCES

- Abrámoff, M.D., Magalhaes, P.J., and Ram, S.J. (2004). Image processing with ImageJ. *Biophotonics Int.* **11**, 36–42.
- Arastu-Kapur, S., Ponder, E.L., Fonović, U.P., Yeoh, S., Yuan, F., Fonović, M., Grainger, M., Phillips, C.I., Powers, J.C., and Bogyo, M. (2008). Identification of proteases that regulate erythrocyte rupture by the malaria parasite *Plasmodium falciparum*. *Nat. Chem. Biol.* **4**, 203–213.
- Benetti, S., De Risi, C., Marchetti, P., Pollini, G.P., and Zanirato, V. (2002). Synthesis of 2,5-disubstituted pyrroles and pyrrolidines by intramolecular cyclization of 6-amino-3-keto sulfones. *Synthesis* **3**, 331–338.
- Böttcher, T., Pitscheider, M., and Sieber, S.A. (2010). Natural products and their biological targets: proteomic and metabolomic labeling strategies. *Angew. Chem. Int. Ed. Engl.* **49**, 2680–2698.
- Chandramohanadas, R., Park, Y., Lui, L., Li, A., Quinn, D., Liew, K., Diez-Silva, M., Sung, Y., Dao, M., Lim, C.T., et al. (2011). Biophysics of malarial parasite exit from infected erythrocytes. *PLoS ONE* **6**, e20869.
- Clerc, J., Florea, B.I., Kraus, M., Groll, M., Huber, R., Bachmann, A.S., Dudler, R., Driessen, C., Overkleeft, H.S., and Kaiser, M. (2009a). Syringolin A selectively labels the 20 S proteasome in murine EL4 and wild-type and bortezomib-adapted leukaemic cell lines. *ChemBioChem* **10**, 2638–2643.
- Clerc, J., Groll, M., Illich, D.J., Bachmann, A.S., Huber, R., Schellenberg, B., Dudler, R., and Kaiser, M. (2009b). Synthetic and structural studies on syringolin A and B reveal critical determinants of selectivity and potency of proteasome inhibition. *Proc. Natl. Acad. Sci. USA* **106**, 6507–6512.
- Clerc, J., Li, N., Krahn, D., Groll, M., Bachmann, A.S., Florea, B.I., Overkleeft, H.S., and Kaiser, M. (2011). The natural product hybrid of Syringolin A and Glidobactin A synergizes proteasome inhibition potency with subsite selectivity. *Chem. Commun. (Camb.)* **47**, 385–387.
- Conroy, T., Guo, J.T., Hunt, N.H., and Payne, R.J. (2010). Total synthesis and antimalarial activity of symplostatins 4. *Org. Lett.* **12**, 5576–5579.
- Conroy, T., Guo, J.T., Lington, R.G., Hunt, N.H., and Payne, R.J. (2011). Total synthesis, stereochemical assignment, and antimalarial activity of gallinamide A. *Chemistry* **17**, 13544–13552.
- Cravatt, B.F., Wright, A.T., and Kozarich, J.W. (2008). Activity-based protein profiling: from enzyme chemistry to proteomic chemistry. *Annu. Rev. Biochem.* **77**, 383–414.
- Deu, E., Leyva, M.J., Albrow, V.E., Rice, M.J., Ellman, J.A., and Bogyo, M. (2010). Functional studies of *Plasmodium falciparum* dipeptidyl aminopeptidase I using small molecule inhibitors and active site probes. *Chem. Biol.* **17**, 808–819.
- Deu, E., Verdoes, M., and Bogyo, M. (2012). New approaches for dissecting protease functions to improve probe development and drug discovery. *Nat. Struct. Mol. Biol.* **19**, 9–16.
- Dondorp, A.M., Nosten, F., Yi, P., Das, D., Phyo, A.P., Tarning, J., Lwin, K.M., Ariey, F., Hanpithakpong, W., Lee, S.J., et al. (2009). Artemisinin resistance in *Plasmodium falciparum* malaria. *N. Engl. J. Med.* **361**, 455–467.
- Drahl, C., Cravatt, B.F., and Sorensen, E.J. (2005). Protein-reactive natural products. *Angew. Chem. Int. Ed. Engl.* **44**, 5788–5809.
- Fonović, M., and Bogyo, M. (2008). Activity-based probes as a tool for functional proteomic analysis of proteases. *Expert Rev. Proteomics* **5**, 721–730.
- Greenbaum, D., Medzihradsky, K.F., Burlingame, A., and Bogyo, M. (2000). Epoxide electrophiles as activity-dependent cysteine protease profiling and discovery tools. *Chem. Biol.* **7**, 569–581.
- Greenbaum, D., Baruch, A., Hayrapetian, L., Darula, Z., Burlingame, A., Medzihradsky, K.F., and Bogyo, M. (2002a). Chemical approaches for functionally probing the proteome. *Mol. Cell. Proteomics* **1**, 60–68.
- Greenbaum, D.C., Baruch, A., Grainger, M., Bozdech, Z., Medzihradsky, K.F., Engel, J., DeRisi, J., Holder, A.A., and Bogyo, M. (2002b). A role for the protease falcipain 1 in host cell invasion by the human malaria parasite. *Science* **298**, 2002–2006.
- Groll, M., Schellenberg, B., Bachmann, A.S., Archer, C.R., Huber, R., Powell, T.K., Lindow, S., Kaiser, M., and Dudler, R. (2008). A plant pathogen virulence factor inhibits the eukaryotic proteasome by a novel mechanism. *Nature* **452**, 755–758.
- Guiguet, W.A., Shelat, A.A., Garcia-Bustos, J.F., Diagona, T.T., Gamo, F.J., and Guy, R.K. (2012). Global phenotypic screening for antimalarials. *Chem. Biol.* **19**, 116–129.
- Harbut, M.B., Velmourougane, G., Dalal, S., Reiss, G., Whisstock, J.C., Onder, O., Brisson, D., McGowan, S., Klemba, M., and Greenbaum, D.C. (2011). Bestatin-based chemical biology strategy reveals distinct roles for malaria M1- and M17-family aminopeptidases. *Proc. Natl. Acad. Sci. USA* **108**, E526–E534.
- Heal, W.P., Dang, T.H., and Tate, E.W. (2011). Activity-based probes: discovering new biology and new drug targets. *Chem. Soc. Rev.* **40**, 246–257.
- Jeffery, D.A., and Bogyo, M. (2003). Chemical proteomics and its application to drug discovery. *Curr. Opin. Biotechnol.* **14**, 87–95.
- Jou, G., González, I., Albericio, F., Lloyd-Williams, P., and Giralt, E. (1997). Total synthesis of dehydrodidemnin B. Use of uronium and phosphonium salt coupling reagents in peptide synthesis in solution. *J. Org. Chem.* **62**, 354–366.
- Kaschani, F., Clerc, J., Krahn, D., Bier, D., Hong, T.N., Ottmann, C., Niessen, S., Colby, T., van der Hoorn, R.A., and Kaiser, M. (2012). Identification of a selective, activity-based probe for glyceraldehyde 3-phosphate dehydrogenases. *Angew. Chem. Int. Ed. Engl.* **51**, 5230–5233.
- Klemba, M., Gluzman, I., and Goldberg, D.E. (2004). A *Plasmodium falciparum* dipeptidyl aminopeptidase I participates in vacuolar hemoglobin degradation. *J. Biol. Chem.* **279**, 43000–43007.
- Kolb, H.C., Finn, M.G., and Sharpless, K.B. (2001). Click chemistry: diverse chemical function from a few good reactions. *Angew. Chem. Int. Ed. Engl.* **40**, 2004–2021.
- Kolodziejek, I., Misas-Villamil, J.C., Kaschani, F., Clerc, J., Gu, C., Krahn, D., Niessen, S., Verdoes, M., Willems, L.I., Overkleeft, H.S., et al. (2011). Proteasome activity imaging and profiling characterizes bacterial effector syringolin A. *Plant Physiol.* **155**, 477–489.
- Lington, R.G., Clark, B.R., Trimble, E.E., Almanza, A., Ureña, L.D., Kyle, D.E., and Gerwick, W.H. (2009). Antimalarial peptides from marine cyanobacteria: isolation and structural elucidation of gallinamide A. *J. Nat. Prod.* **72**, 14–17.
- Lomenick, B., Olsen, R.W., and Huang, J. (2011). Identification of direct protein targets of small molecules. *ACS Chem. Biol.* **6**, 34–46.
- Mayer, A.M., Glaser, K.B., Cuevas, C., Jacobs, R.S., Kem, W., Little, R.D., McIntosh, J.M., Newman, D.J., Potts, B.C., and Shuster, D.E. (2010). The odyssey of marine pharmaceuticals: a current pipeline perspective. *Trends Pharmacol. Sci.* **31**, 255–265.

- Méthot, N., Guay, D., Rubin, J., Ethier, D., Ortega, K., Wong, S., Normandin, D., Beaulieu, C., Reddy, T.J., Riendeau, D., and Percival, M.D. (2008). In vivo inhibition of serine protease processing requires a high fractional inhibition of cathepsin C. *Mol. Pharmacol.* **73**, 1857–1865.
- Millholland, M.G., Chandramohanadas, R., Pizzarro, A., Wehr, A., Shi, H., Darling, C., Lim, C.T., and Greenbaum, D.C. (2011). The malaria parasite progressively dismantles the host erythrocyte cytoskeleton for efficient egress. *Mol. Cell. Proteomics* **10**, M111.010678.
- Moura, P.A., Dame, J.B., and Fidock, D.A. (2009). Role of *Plasmodium falciparum* digestive vacuole plasmepsins in the specificity and antimalarial mode of action of cysteine and aspartic protease inhibitors. *Antimicrob. Agents Chemother.* **53**, 4968–4978.
- Nogueira, C.R., and Lopes, L.M.X. (2011). Antiplasmodial natural products. *Molecules* **16**, 2146–2190.
- Pandey, K.C., Singh, N., Arastu-Kapur, S., Bogyo, M., and Rosenthal, P.J. (2006). Falstatin, a cysteine protease inhibitor of *Plasmodium falciparum*, facilitates erythrocyte invasion. *PLoS Pathog.* **2**, e117.
- Patino, N., Frerot, E., Galeotti, N., Poncet, J., Coste, J., Dufour, M.N., and Jouin, P. (1992). Total synthesis of the proposed structure of Dolastatin-15. *Tetrahedron* **48**, 4115–4122.
- Powers, J.C., Asgian, J.L., Ekici, O.D., and James, K.E. (2002). Irreversible inhibitors of serine, cysteine, and threonine proteases. *Chem. Rev.* **102**, 4639–4750.
- Rix, U., and Superti-Furga, G. (2009). Target profiling of small molecules by chemical proteomics. *Nat. Chem. Biol.* **5**, 616–624.
- Rosenthal, P.J. (2004). Cysteine proteases of malaria parasites. *Int. J. Parasitol.* **34**, 1489–1499.
- Rosenthal, P.J. (2011). Falcipains and other cysteine proteases of malaria parasites. *Adv. Exp. Med. Biol.* **712**, 30–48.
- Rosenthal, P.J., McKerrow, J.H., Aikawa, M., Nagasawa, H., and Leech, J.H. (1988). A malarial cysteine proteinase is necessary for hemoglobin degradation by *Plasmodium falciparum*. *J. Clin. Invest.* **82**, 1560–1566.
- Sijwali, P.S., and Rosenthal, P.J. (2004). Gene disruption confirms a critical role for the cysteine protease falcipain-2 in hemoglobin hydrolysis by *Plasmodium falciparum*. *Proc. Natl. Acad. Sci. USA* **101**, 4384–4389.
- Sijwali, P.S., Kato, K., Seydel, K.B., Gut, J., Lehman, J., Klemba, M., Goldberg, D.E., Miller, L.H., and Rosenthal, P.J. (2004). *Plasmodium falciparum* cysteine protease falcipain-1 is not essential in erythrocytic stage malaria parasites. *Proc. Natl. Acad. Sci. USA* **101**, 8721–8726.
- Sijwali, P.S., Koo, J., Singh, N., and Rosenthal, P.J. (2006). Gene disruptions demonstrate independent roles for the four falcipain cysteine proteases of *Plasmodium falciparum*. *Mol. Biochem. Parasitol.* **150**, 96–106.
- Speers, A.E., Adam, G.C., and Cravatt, B.F. (2003). Activity-based protein profiling in vivo using a copper(I)-catalyzed azide-alkyne [3 + 2] cycloaddition. *J. Am. Chem. Soc.* **125**, 4686–4687.
- Taori, K., Liu, Y., Paul, V.J., and Luesch, H. (2009). Combinatorial strategies by marine cyanobacteria: symplostatin 4, an antimitotic natural dolastatin 10/15 hybrid that synergizes with the coproduced HDAC inhibitor largazole. *ChemBioChem* **10**, 1634–1639.
- Teixeira, C., Gomes, J.R., and Gomes, P. (2011). Falcipains, *Plasmodium falciparum* cysteine proteases as key drug targets against malaria. *Curr. Med. Chem.* **18**, 1555–1572.
- van der Hooft, R.A., Leeuwenburgh, M.A., Bogyo, M., Joosten, M.H., and Peck, S.C. (2004). Activity profiling of papain-like cysteine proteases in plants. *Plant Physiol.* **135**, 1170–1178.
- Wang, F., Krai, P., Deu, E., Bibb, B., Lauritzen, C., Pedersen, J., Bogyo, M., and Klemba, M. (2011). Biochemical characterization of *Plasmodium falciparum* dipeptidyl aminopeptidase 1. *Mol. Biochem. Parasitol.* **175**, 10–20.
- Wells, T.N., Alonso, P.L., and Gutteridge, W.E. (2009). New medicines to improve control and contribute to the eradication of malaria. *Nat. Rev. Drug Discov.* **8**, 879–891.
- World Health Organization (2011). World Malaria Report 2011 (http://www.who.int/malaria/world_malaria_report_2011/en/).